

## Dynamics of Water Molecules in Glucose Solutions

César Talon<sup>†</sup>

*Centre de Recherche sur la Matière Divisée, 45071 Orléans Cedex 2, France*

Luis J. Smith<sup>‡</sup>

*Argonne National Laboratory, Argonne, Illinois 60439*

John W. Brady and Bertha A. Lewis

*Department of Food Sciences, Cornell University, Ithaca, New York 14853*

John R. D. Copley

*NIST Center for Neutron Research, National Institute of Standards and Technology, Gaithersburg, Maryland 20899*

David L. Price\*

*Centre de Recherche sur les Matériaux à Haute Température, 45071 Orléans Cedex 2, France*

Marie-Louise Saboungi

*Centre de Recherche sur la Matière Divisée, 45071 Orléans Cedex 2, France*

*Received: April 30, 2003; In Final Form: February 19, 2004*

The effects of the solution of glucose molecules on the dynamics of solvent water have been studied by quasielastic neutron scattering (QENS) measurements on solutions of selectively deuterated glucose in natural water. The data are fitted to two Lorentzians ascribed to pure translational and mixed translational and rotational character, respectively. The addition of the glucose to the water causes a substantial slowing down, by a factor 10 for the translational diffusion and 3–4 for the rotational motion at the highest concentration studied, 1:11 C<sub>6</sub>H<sub>12</sub>O<sub>6</sub>:H<sub>2</sub>O. The values obtained for water diffusion constants are consistent with previous QENS and NMR experiments on monosaccharide solutions but an order of magnitude higher than those derived from a recent molecular dynamics simulation.

### I. Introduction

Hydrated sugars are ubiquitous in living systems, not only as a metabolic currency but also in many other roles, such as mediators in molecular recognition processes. The effects of sugars on the structure and dynamics of water in these systems can often be quite important and are receiving increasing attention. For example, the glass transition temperatures of the various sugars have been found to vary considerably as a function of sugar stereochemistry, with the cryoprotectants trehalose and sucrose having the highest  $T_g$ 's, but a general theory of the relationship between sugar structure and  $T_g$  is not available. Characterizing the dynamics of water molecules in sugar solutions would not only be directly useful but would also be helpful in developing a general understanding of the effects of all types of biological solutes on water. The simple sugars can serve as general models for the study of the structure and dynamics of water in aqueous biological solutions for

several reasons. Not only are they small and relatively regular in structure, containing only three types of atoms, but the functional groups found in sugars also occur in proteins and nucleic acids. They are quite soluble in water, even at high concentrations, and unlike peptides and nucleotides, they generally exist in only one conformation at room temperature. Although they are structural isomers of one another, the different simple sugars have differing physical properties in solution, determined by the details of the interactions of the sugars with the solvent and the way that these interactions vary with the spatial topology of the functional groups.

The polyfunctional, hydrogen-bonding carbohydrates would be expected to interact strongly with aqueous solvent. The organization of water molecules around a particular solute will in general involve both positional and orientational correlations with the specific chemical architecture of the solute and thus will vary in its details from one molecule to the next. For carbohydrates, this solvent structuring can be quite complex, due to their complicated mix of chemical functionalities, with hydrogen bonding and nonpolar functional groups, each with its own specific hydration requirements, in close proximity to one another. Recent MD simulations of hydrated sugars in dilute solutions<sup>1–3</sup> have suggested that water molecules can become

\* To whom correspondence should be addressed. E-mail: price@cnrs-orleans.fr.

<sup>†</sup> Present address: Department of Food Sciences, Cornell University, Ithaca, NY 14853.

<sup>‡</sup> Present address: Carlson School of Chemistry, Clark University, Worcester, MA 01610.

highly localized at specific positions around sugar solutes, but the effects of such structuring on rotational and translational motions of the water have not yet been fully characterized computationally.<sup>4</sup> Any such effects should become much more pronounced at higher concentrations as these hydration shells began to overlap. Recently, we reported the use of quasielastic neutron scattering experiments (QENS) to characterize glucose diffusion in concentrated solutions. In those studies, the nature of glucose diffusion was found to undergo a transition from continuous to jump diffusion as a function of concentration in the range from 1 to 5 molal at low temperatures, perhaps as a result of the transient development of a hydrogen-bonded network of glucose and water at the highest concentration. In the present work, we focus on the inverse problem, the effects of the solution of glucose molecules on the dynamics of the solvent water.

Selective H:D isotope substitution is a valuable tool for sorting out the dynamics of a complex organic system with QENS. Since the total bound-atom scattering cross section for H (81.7 b) is much larger than that of D (7.6 b) and most other atoms, the measured intensity is dominated by the scattering from the H atoms. Moreover the scattering from H is 98% incoherent so that the complicating effects of interference in the scattering between different atoms can generally be neglected. In a companion set of experiments, the diffusion rates, jump times, and rotational relaxation times for natural glucose in deuterated water at molar ratios of 1:11, 1:20, and 1:55 have been determined.<sup>5</sup> In the present work, we focus on the inverse problem, the effects of the solution of glucose molecules on the dynamics of the solvent water, studied by dissolving selectively deuterated glucose in natural water at the same molar ratios. The experimental situation is complicated by the unavoidable exchange of 5 of the 12 D atoms of the glucose molecule by H from the solvent water, so that some contribution to the scattering from the glucose is inevitable. A sample with only two D atoms on the nonexchangeable sites was measured in order to investigate the importance of this effect. In addition, a sample of the  $\alpha$ -methyl glycoside of 1d<sub>2</sub>-D-glucose was prepared and studied in order to freeze out the process of anomeric equilibration. Free hemiacetal sugars in water continually undergo tautomeric conversion, which in the case of D-glucose produces a 64%  $\beta$ /36%  $\alpha$  mixture of the two anomers. By preparing the methyl glycoside and isolating the  $\alpha$  anomer only, the diffusional properties of a single chemical species could be studied.

## II. Experimental Section

The following samples were prepared:

- (1) pure water, as a reference point;
- (2–4) solutions of 7d-glucose (D-glucose, C<sub>6</sub>H<sub>12</sub>O<sub>6</sub>, deuterated at the C<sub>1</sub>, C<sub>2</sub>, C<sub>3</sub>, C<sub>4</sub>, C<sub>5</sub> and twice at the C<sub>6</sub> position) in light water at molar concentrations of 1:55, 1:20 and 1:11 C<sub>6</sub>H<sub>12</sub>O<sub>6</sub>:H<sub>2</sub>O (we will refer to these solutions as *glu55*, *glu20*, and *glu11*): these concentrations would correspond to 15.4, 33.3 and 47.6 wt %, respectively, in fully protonated solutions;
- (5) 2d<sub>66</sub>-glucose (deuterated twice at the C<sub>6</sub> position) at the 1:11 molar concentration (*d<sub>66</sub>glu11*);
- (6) 1d<sub>2</sub>-glucose, deuterated at the C2 position and methylated at the anomeric C1 position, at the 1:11 molar concentration (*mglu11*).

In the case of samples 2–4, fully deuterated glucose was mixed with light water, dried and re-mixed with light water to avoid deuteration of the water by exchangeable hydrogens. The samples were loaded into aluminum annular cans with an

**TABLE 1: Relative Contributions to the Incoherent and Coherent Scattering from Glucose and Water**

| sample                | incoherent scattering             |                                 | coherent scattering               |                                 |
|-----------------------|-----------------------------------|---------------------------------|-----------------------------------|---------------------------------|
|                       | glucose contribution <sup>a</sup> | water contribution <sup>a</sup> | glucose contribution <sup>a</sup> | water contribution <sup>a</sup> |
| water                 |                                   | 53.27                           |                                   | 2.58                            |
| glu55                 | 2.19                              | 46.51                           | 0.56                              | 2.26                            |
| glu20                 | 4.93                              | 38.05                           | 1.27                              | 1.85                            |
| glu11                 | 7.26                              | 30.84                           | 1.87                              | 1.50                            |
| d <sub>66</sub> glu11 | 14.09                             | 30.84                           | 1.53                              | 1.50                            |
| mglu11                | 18.26                             | 29.30                           | 1.55                              | 1.42                            |

<sup>a</sup> Scattering cross section (barns) averaged over all atoms in the sample.

annular distance of 0.1 mm and placed within the radiation shield of a closed-cycle refrigerator, in which the temperature could be controlled to  $\pm 1$  K.

QENS experiments were carried out on the Disk Chopper Spectrometer<sup>6</sup> at the NIST Center for Neutron Research at an incident wavelength of 6.0 Å. The time-of-flight of the scattered neutrons was measured in 18 groups of detectors at scattering angles ranging from 5° to 140°, corresponding to wave vector transfers for elastic scattering from 0.25 to 1.93 Å<sup>-1</sup>. Runs of approximately 3 h were made at temperatures of 280, 300, and 320 K, except for water, which was measured only at 280 K and sample 7 at 280 and 320 K. The contributions to the incoherent and coherent scattering from the sugar and the water are given in Table 1. At low  $Q$  the scattering is dominated by the incoherent terms, but at the higher  $Q$  values measured here, the coherent terms will be significant. The total scattering probabilities can be obtained by multiplying the total scattering cross sections in Table 1 by 0.002, so that, e.g., the water sample represents an 11% scatterer. This is a rough measure of the ratio of multiple to single scattering.

The measured QENS spectra were corrected for container scattering and analyzed to give scattering functions  $S(Q, E)$ , where  $Q$  denotes the modulus of the scattering vector and  $E$  the energy transfer. The resolution function determined from a measurement with a vanadium standard was approximately Gaussian in shape with a full width at half-maximum (fwhm) of 0.055 meV. Various combinations of theoretical functions, Lorentzian, delta, and the Fourier transform of a stretched-exponential time decay,<sup>7</sup> were convoluted with the resolution function and fitted to the experimental  $S(Q, E)$  by nonlinear least-squares fitting. Feeney et al.<sup>8</sup> reported that a stretched-exponential function and a delta function plus Lorentzian gave roughly equivalent fits to QENS results on fructose. In the present experiment, the stretched-exponential function gave an adequate fit for the 1:11 concentration but not for the lower concentrations or for water. A combination of two Lorentzian lines with a linear background produced the best overall fits to our results at the various concentrations and temperatures measured. They were not substantially improved by the addition of a delta-function, and we eliminated the latter in order to keep the number of fitting parameters as low as possible. Two typical fits are shown in Figure 1.

## III. Results

The measured scattering functions were fitted by the expression

$$S(Q, E) = c_1(Q)\mathcal{L}(W_1, E) + c_2(Q)\mathcal{L}(W_2, E) + a + bE \quad (1)$$

where  $\mathcal{L}(W, E)$  denotes a Lorentzian function with unit area and

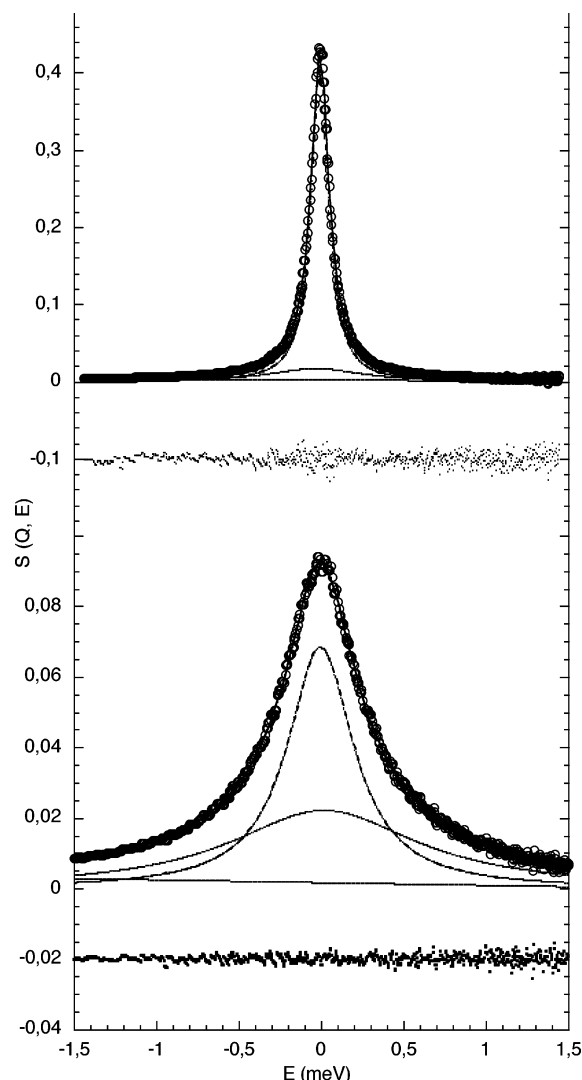


**Figure 1.** Typical fits of two Lorentzian functions and a sloping background to the QENS data, in this case for the glu55 sample at 300 K at  $Q = 0.72 \text{ \AA}^{-1}$  (upper figure) and  $1.76 \text{ \AA}^{-1}$  (lower figure). The residuals, defined as (data-fit)/(standard deviation), are shown below each figure, multiplied by 0.01 in the upper figure and 0.002 in the lower.

full width at half-maximum (fwhm)  $W$  and the linear background terms allow for a slowly varying inelastic scattering component. The values obtained for  $W_1$  and  $W_2$  as a function of scattering vector  $Q$  are plotted in Figures 2 and 3 for the six samples at 280 K. In Figure 3, the large scatter at low  $Q$  reflects the fact that the intensity should go to zero at  $Q = 0$ , as illustrated in Figure 1 and discussed in the next section. Figure 4 shows the temperature dependence of  $W_1$  and  $W_2$  for the 1:11 7d-glucose solution.

The  $Q$  dependence of the  $W_n$  was least-squares-fitted by the following expressions:

$$W_1 = \alpha_1 + \beta_1 Q^2 / (1 + \gamma_1 Q^2) \quad (2a)$$

$$W_2 = \alpha_2 + \beta_2 Q^2 \quad (2b)$$

The form taken for eq 2a anticipates the model discussed in the next section, whereas that of eq 2b was chosen empirically. The fitted functions are shown as continuous lines in Figures 2–4, and the values of the parameters are given in Table 2.

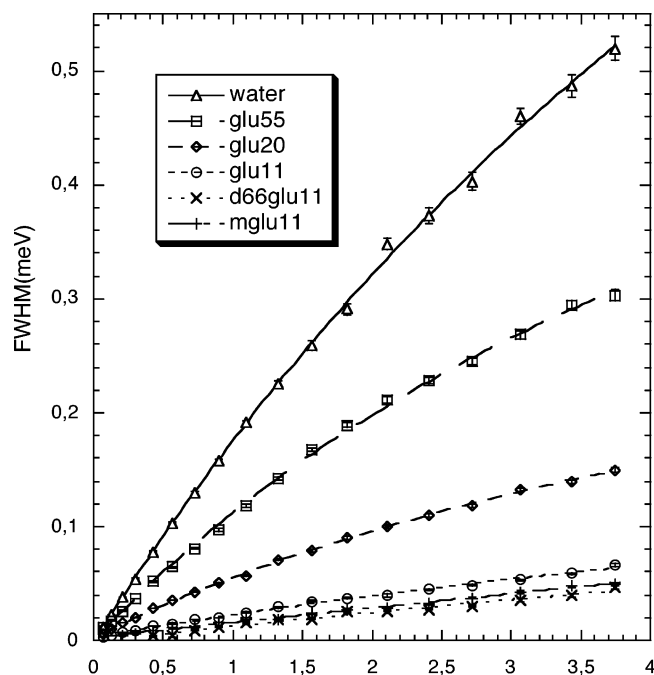


**Figure 2.** Full-width at half-maximum,  $W_1$ , of the narrower Lorentzian fitted to the QENS spectra measured in water and glucose-water solutions at 280 K. The lines represent fits of eq 2a. The sample designations in the legend are defined in section II.

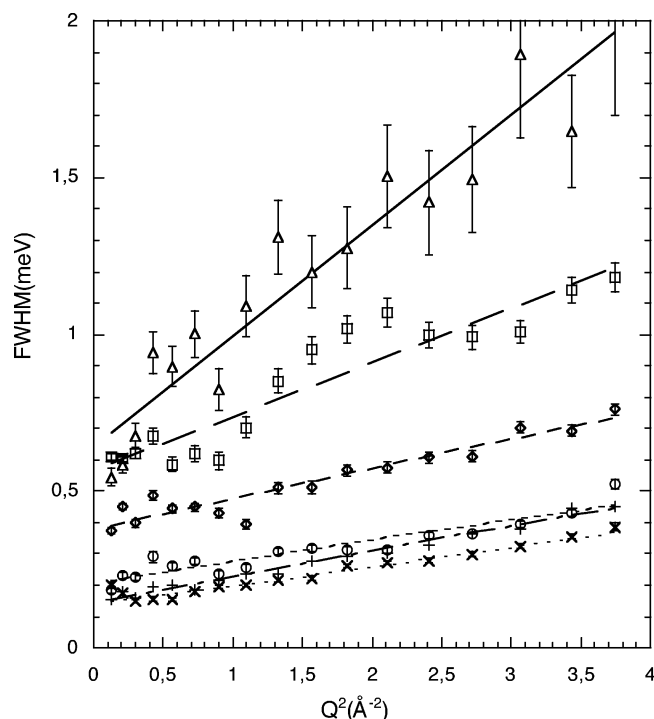


**Figure 3.** Full-width at half-maximum,  $W_2$ , of the broader Lorentzian fitted to the QENS spectra at 280 K. The lines represent fits of eq 2b. Notation as in Figure 2.

#### IV. Analysis and Discussion

**A. Theoretical Considerations.** The well-known model of Teixeira et al. (TBCD) for water<sup>9</sup> provides a framework for analyzing and interpreting our results. In this model, the observed scattering is represented by a product of intermediate scattering functions  $I_i(Q, t)$  or alternatively by a convolution of scattering functions  $S_i(Q, E)$ , corresponding to vibrational, translational, and rotational degrees of freedom. In the quasielastic

TABLE 2: Parameters Fitted to  $W_1$  and  $W_2$ 

| sample                | $T$ (K)             | $\alpha_1$ (meV)    | $\beta_1$ (meV $\text{\AA}^2$ ) | $\gamma_1$ ( $\text{\AA}^2$ ) | $\alpha_2$ (meV)  | $\beta_2$ (meV $\text{\AA}^2$ ) |
|-----------------------|---------------------|---------------------|---------------------------------|-------------------------------|-------------------|---------------------------------|
| water                 | 280                 | $-0.001 \pm 0.003$  | $0.196 \pm 0.006$               | $0.11 \pm 0.01$               | $0.64 \pm 0.05$   | $0.35 \pm 0.03$                 |
| glu55                 | 280                 | $0.000 \pm 0.002$   | $0.129 \pm 0.004$               | $0.15 \pm 0.01$               | $0.57 \pm 0.03$   | $0.17 \pm 0.02$                 |
| "                     | 300                 | $-0.002 \pm 0.006$  | $0.21 \pm 0.01$                 | $0.13 \pm 0.002$              | $0.65 \pm 0.08$   | $0.32 \pm 0.04$                 |
| "                     | 320                 | $0.002 \pm 0.007$   | $0.29 \pm 0.01$                 | $0.07 \pm 0.01$               | $0.58 \pm 0.09$   | $0.63 \pm 0.05$                 |
| "                     | 280 (refined)       |                     | $0.130 \pm 0.004$               |                               | $0.57 \pm 0.03$   | $0.17 \pm 0.02$                 |
| "                     | $E_a/k$ ( $10^3$ K) |                     | $1.8 \pm 0.1$                   |                               | $0.2 \pm 0.3$     | $3.0 \pm 0.3$                   |
| glu20                 | 280                 | $0.0033 \pm 0.0008$ | $0.059 \pm 0.002$               | $0.14 \pm 0.01$               | $0.38 \pm 0.01$   | $0.095 \pm 0.008$               |
| "                     | 300                 | $0.007 \pm 0.002$   | $0.090 \pm 0.003$               | $0.09 \pm 0.01$               | $0.42 \pm 0.03$   | $0.16 \pm 0.01$                 |
| "                     | 320                 | $0.000 \pm 0.009$   | $0.17 \pm 0.02$                 | $0.21 \pm 0.06$               | $0.52 \pm 0.05$   | $0.17 \pm 0.03$                 |
| "                     | 280 (refined)       |                     | $0.058 \pm 0.002$               |                               | $0.38 \pm 0.01$   | $0.100 \pm 0.008$               |
| "                     | $E_a/k$ ( $10^3$ K) |                     | $1.9 \pm 0.2$                   |                               | $0.6 \pm 0.2$     | $1.7 \pm 0.3$                   |
| glu11                 | 280                 | $0.0030 \pm 0.0008$ | $0.021 \pm 0.001$               | $0.08 \pm 0.02$               | $0.21 \pm 0.01$   | $0.067 \pm 0.006$               |
| "                     | 300                 | $0.004 \pm 0.001$   | $0.038 \pm 0.002$               | $0.08 \pm 0.02$               | $0.25 \pm 0.01$   | $0.104 \pm 0.007$               |
| "                     | 320                 | $0.006 \pm 0.002$   | $0.061 \pm 0.004$               | $0.08 \pm 0.02$               | $0.26 \pm 0.01$   | $0.167 \pm 0.007$               |
| "                     | 280 (refined)       |                     | $0.0211 \pm 0.0009$             |                               | $0.215 \pm 0.009$ | $0.065 \pm 0.005$               |
| "                     | $E_a/k$ ( $10^3$ K) |                     | $2.4 \pm 0.2$                   |                               | $0.5 \pm 0.1$     | $2.1 \pm 0.2$                   |
| d <sub>66</sub> glu11 | 280                 | $-0.001 \pm 0.002$  | $0.014 \pm 0.003$               | $0.06 \pm 0.06$               | $0.143 \pm 0.007$ | $0.060 \pm 0.004$               |
| "                     | 300                 | $0.005 \pm 0.003$   | $0.025 \pm 0.004$               | $0.02 \pm 0.05$               | $0.19 \pm 0.01$   | $0.098 \pm 0.005$               |
| "                     | 320                 | $0.005 \pm 0.003$   | $0.057 \pm 0.005$               | $0.10 \pm 0.03$               | $0.24 \pm 0.02$   | $0.173 \pm 0.008$               |
| "                     | 280 (refined)       |                     | $0.0124 \pm 0.002$              |                               | $0.143 \pm 0.007$ | $0.058 \pm 0.003$               |
| "                     | $E_a/k$ ( $10^3$ K) |                     | $3.4 \pm 0.5$                   |                               | $1.1 \pm 0.2$     | $2.4 \pm 0.2$                   |
| mglu11                | 280                 | $0.0030 \pm 0.0007$ | $0.0129 \pm 0.0009$             | $0.01 \pm 0.02$               | $0.140 \pm 0.005$ | $0.081 \pm 0.003$               |
| "                     | 320                 | $0.008 \pm 0.002$   | $0.052 \pm 0.003$               | $0.08 \pm 0.02$               | $0.28 \pm 0.01$   | $0.154 \pm 0.007$               |
| "                     | $E_a/k$ ( $10^3$ K) |                     | $3.1 \pm 0.5$                   |                               | $1.6 \pm 0.2$     | $1.4 \pm 0.2$                   |

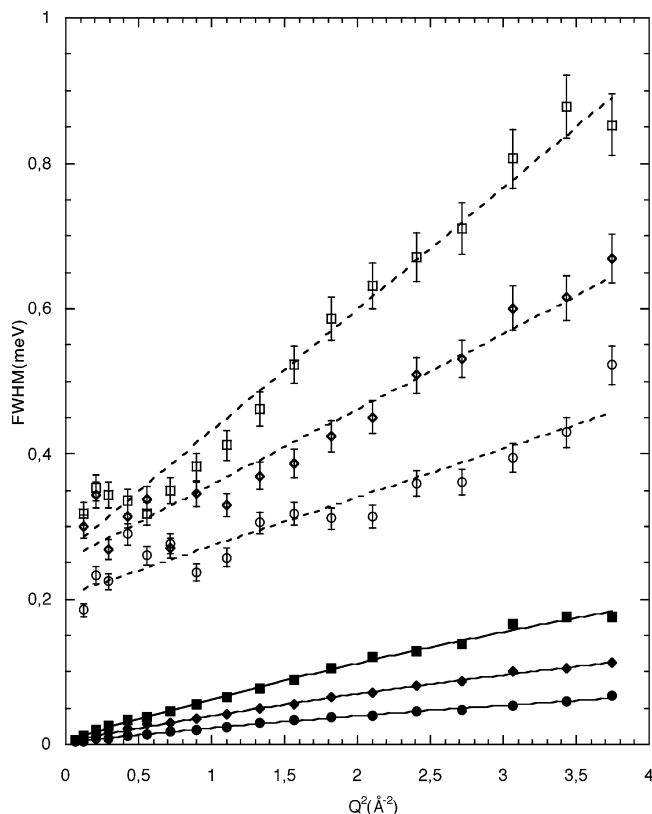


**Figure 4.** Values of  $W_1$  (solid symbols) and  $W_2$  (open symbols) for the glu11 solution at 280 K (circles), 300 K (diamonds), and 320 K (squares). The solid and dotted lines represent fits of eqs 2a and 2b.

region of interest here, the vibrational function is represented by a Debye–Waller factor. The translational scattering function is represented in the incoherent approximation and rapid jump diffusion model<sup>10</sup> as  $\mathcal{L}(W_t, E)$  with fwhm given by

$$W_t = \frac{2\hbar D Q^2}{1 + l^2 Q^2/6} \quad (3)$$

where  $D$  is the diffusion constant and  $l$  is an effective jump

distance. Following the treatment of Sears<sup>11</sup> for freely rotating molecules, the rotational scattering function is expressed as the sum of a delta function and a series of Lorentzians

$$S_{\text{rot}}(Q, E) = A_0 \delta(E) + \sum_{l=1}^{\infty} A_l(Q) \mathcal{L}(W_{rl}, E) \quad (4a)$$

with

$$A_l(Q) = (2l + 1) j_l^2(a_m Q) \quad (4b)$$

where  $a_m$  is an effective molecular radius, and

$$W_{rl} = \frac{\hbar l(l + 1)}{3\tau} \quad (4c)$$

$\tau$  being a relaxation time for orientational diffusion. Thus, the total incoherent structure factor can be written

$$S^{\text{inc}}(Q, E) = \exp(-\langle u^2 \rangle Q^2) \{ A_0(Q) \mathcal{L}(W_t, E) + \sum_{l=1}^{\infty} A_l(Q) \mathcal{L}(W_t + W_{rl}, E) \} \quad (5)$$

Since  $a_m = 1.0 \text{ \AA}$  for water,  $a_m Q \leq 2$  for this experiment and the  $A_l(Q)$  decrease rapidly with  $l$ . Teixeira et al. included the first three terms of eq 5 in fitting their model to data taken out to  $Q = 2 \text{ \AA}^{-1}$ . If we identify the quasielastic terms in eq 1 with eq 5,  $\mathcal{L}(W_1, E)$  corresponds to  $\mathcal{L}(W_t, E)$  and thus  $W_1$  with  $W_t$ . Comparison of eq 2a with eq 3 then implies that

$$\alpha_1 = 0 \quad (6a)$$

$$\beta_1 = 2\hbar D \quad (6b)$$

$$\gamma_1 = l^2/6 \quad (6c)$$

Considering the following terms,  $\mathcal{L}(W_2, E)$  can be associated with  $\mathcal{L}(W_t + W_{r1}, E)$  at low  $Q$ , with an admixture of the  $l = 2$

terms as  $Q$  increases. Thus, comparison of eq 2b with eqs 3 and 4c implies that

$$\alpha_2 = \frac{2\hbar}{3\tau} \quad (7)$$

and  $\beta_2$  will have two compensating components, one that is identified with  $2\hbar D$  and another reflecting the increasing contribution of the higher  $l$  terms of eq 5 as  $Q$  increases.

Comparison of our results for water at 280 K with the TBCD model provides a check on the reliability of our analysis procedure. We took the TBCD parameters interpolated to a temperature of 280 K, added a multiple scattering component estimated as 10% of the scattering observed at the highest  $Q$ , and fitted eq 1 over the  $(Q, E)$  range of our measurement. The resulting values for  $\alpha_1$ ,  $\beta_1$ ,  $\gamma_1$ , and  $\alpha_2$  were  $0.008 \pm 0.007$ ,  $0.15 \pm 0.01$ ,  $0.16 \pm 0.03$ , and  $0.48 \pm 0.03$ , respectively, compared with the TBCD values of 0, 0.177, 0.28, and 0.325. From this, we conclude that our fitted values for  $\beta_1$  are reliable to within 20% but that  $\gamma_1$  is underestimated and  $\alpha_2$  is overestimated, by about 50%. The small nonzero values of  $\alpha_1$  must result from small differences in the resolution function compared with the vanadium standard and possibly also from broadening due to rotational motions of the sugar molecules. The problem with the rotational term  $\alpha_2$  appears to stem from the difficulty of measuring a relatively broad and (at low  $Q$ ) small component in the presence of a narrow component and significant (10–12%) multiple scattering.

The comparison of the amplitude factors in eqs 1 and 5 implies that

$$c_1 = \exp(-\langle u^2 \rangle Q^2) A_0(Q) \quad (8a)$$

and

$$c_2 = \exp(-\langle u^2 \rangle Q^2) \sum_{l=1}^{\infty} A_l(Q) \quad (8b)$$

so that at lower  $Q$  (before the higher components in eq 7b fall out of the window of the quasielastic fit), the measurement of absolute values of  $c_1$  and  $c_2$  provide in principle the means of determining  $A_0(Q)$  (hence a measure of  $a_m$ ) and the Debye–Waller factor  $\exp(-\langle u^2 \rangle Q^2)$ . In the present work, we have not been able to obtain reliable results for these quantities, due to complications arising from the higher components in eq 8b.

**B. Translational Dynamics.** The values of the translation diffusion parameter  $\beta_1$ , plotted in Figure 5 as a function of  $1000/T(K)$ , exhibit an Arrhenius dependence. The Arrhenius fits yield refined estimates for the values at 280 K, taken as the reference temperature, and for the activation energies, also given in Table 2. The value of  $\beta_1$  obtained for pure water,  $0.196 \pm 0.006$  meV  $\text{\AA}^2$ , corresponds to  $D = (1.49 \pm 0.15) \times 10^{-5}$  cm<sup>2</sup> s<sup>-1</sup>, in agreement with the interpolated TBCD value,  $1.34 \times 10^{-5}$  cm<sup>2</sup> s<sup>-1</sup>.<sup>9</sup> As the 7d-glucose concentration is increased,  $\beta_1$  falls systematically down to a value corresponding to  $D = (0.160 \pm 0.015) \times 10^{-5}$  cm<sup>2</sup> s<sup>-1</sup> at the 1:11 concentration, almost 10 times lower than the value for water. This change reflects principally the effect of the glucose in slowing down the dynamics of the water molecules, since even at the 1:11 concentration the sugar is contributing only about 20% of the total scattering (Table 1). Moreover, the dynamics of the glucose molecules are four times slower, corresponding to a diffusion constant of  $4.5 \times 10^{-7}$  cm<sup>2</sup> s<sup>-1</sup> at 280 K as determined from the measurements on natural glucose in D<sub>2</sub>O.<sup>5</sup> The small further reduction in  $\beta_1$  with the more hydrogenated sugar molecules,

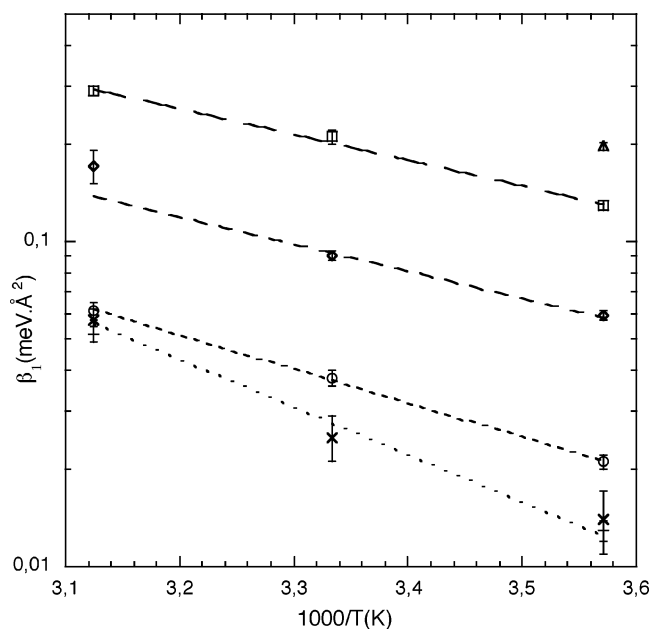


**Figure 5.** Values of  $\beta_1$  derived from the fits of eq 2a. The lines represent Arrhenius fits. Notation as in Figure 2.

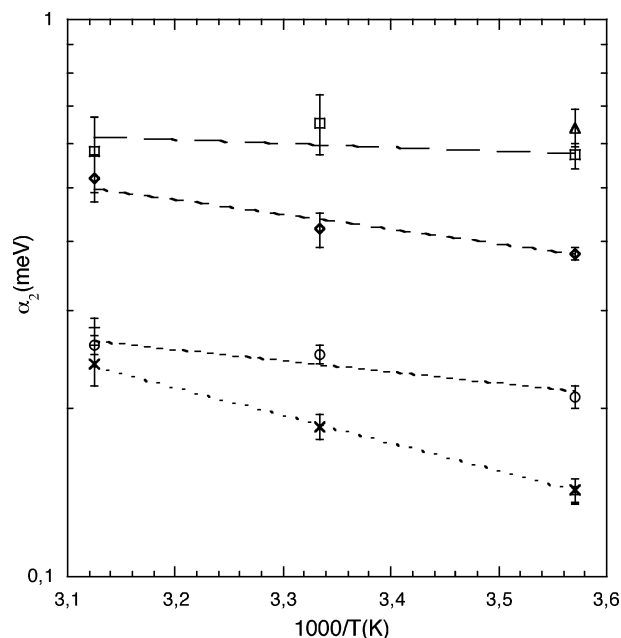


**Figure 6.** Values of  $\alpha_2$  derived from the fits of eq 2b. The lines represent Arrhenius fits. Notation as in Figure 2.

2d<sub>66</sub>-glucose and 1d<sub>2</sub>-methylated glucose, may reflect the increased contribution of the sugar to the scattering and thus give an indication of the magnitude of this contribution in the case of the 7d-glucose. We do not see a significant difference in the diffusional behavior of the single isomer of methylated glucose and the mixture of two isomers of unmethylated glucose. The temperature dependence of  $\beta_1$  for the glucose solutions gives an average activation energy for diffusion that appears to increase with sugar concentration; the average value for the two lower concentrations is  $3.7 \pm 0.3$  kcal mol<sup>-1</sup>, similar to the TBCD value for water, 3.6 kcal mol<sup>-1</sup>.<sup>9</sup>

**C. Rotational Dynamics.** The values of  $\alpha_2$  are plotted in Figure 6 against  $1000/T(K)$ . For pure water at 280 K,  $\alpha_2 = 0.64 \pm 0.05$  meV; as discussed above, this is expected to be an over-estimate, and the derived value of  $\tau$ ,  $0.69 \pm 0.05$  ps, is indeed lower than the TBCD value of 1.35 ps.<sup>5</sup> As the



**TABLE 3: Comparison of Water Diffusion Constants and Activation Energies in Monosaccharide Solutions with Values in the Literature**

| reference<br>(technique)                          | sugar, wt %   | <i>T</i><br>(K) | <i>D</i> (H <sub>2</sub> O)<br>(10 <sup>-5</sup> cm <sup>2</sup> /s) | <i>E<sub>a</sub>D</i> (H <sub>2</sub> O)<br>(kcal/mol) |
|---|---------------|-----------------|--|--|
| this work<br>(QENS)                               | water         | 280             | 1.49 ± 0.05  |  |
|   | glucose, 15%  | 280             | 0.98 ± 0.03  | 3.6 ± 0.2  |
|   | glucose, 33%  | 280             | 0.44 ± 0.02  | 3.8 ± 0.4  |
|   | glucose, 48%  | 280             | 0.160 ± 0.007  | 4.8 ± 0.4  |
|   | glucose, 15%  | 300             | 1.59 ± 0.08  |  |
|   | glucose, 33%  | 300             | 0.68 ± 0.02  |  |
|   | glucose, 48%  | 300             | 0.29 ± 0.02  |  |
|   | glucose, 15%  | 320             | 2.20 ± 0.08  |  |
|   | glucose, 33%  | 320             | 1.3 ± 0.2  |  |
|   | glucose, 48%  | 320             | 0.46 ± 0.03  |  |
| ref 8<br>(QENS)                                   | water         | 300             | 2.67 ± 0.05  |  |
|   | fructose, 4%  | 300             | 2.5 ± 0.1  |  |
|   | fructose, 29% | 300             | 1.8 ± 0.1  |  |
| ref 14<br>( <sup>2</sup> H NMR)                   | fructose, 60% | 300             | 0.7 ± 0.2  |  |
|   | glucose, 40%  | 280             | 0.20 ± 0.02  | 6.11 ± 0.07  |
|   | glucose, 75%  | 280             | 0.03 ± 0.01  | 7.5 ± 0.2  |
|   | glucose, 40%  | 300             | 0.42 ± 0.04  |  |
| ref 15<br>( <sup>1</sup> H & <sup>13</sup> C NMR) | glucose, 75%  | 300             | 0.07 ± 0.03  |  |
|   | fructose, 30% | 298             | 1.57   | 4.1  |
|   | fructose, 50% | 298             | 0.65   | 4.8  |
|   | fructose, 70% | 298             | 0.22   | 5.6  |
| ref 4<br>(MD)                                     | water         | 270             | 1.7 ± 0.1  | 2.2 ± 0.1  |
|   | glucose, 4%   | 270             | 0.63 ± 0.07  | 5.6 ± 0.06   |
|   | glucose, 29%  | 270             | 0.018 ± 0.005  | 9.6 ± 0.09   |
|   | water         | 300             | 2.58 ± 0.03  |  |
|   | glucose, 4%   | 300             | 1.80 ± 0.08  |  |
|   | glucose, 29%  | 300             | 0.107 ± 0.007  |  |
|   | glucose, 60%  | 300             | 0.018 ± 0.002  |  |
|   | fructose, 4%  | 300             | 1.80 ± 0.05  |  |
|   | fructose, 29% | 300             | 0.062 ± 0.005  |  |
|   | fructose, 60% | 300             | 0.016 ± 0.003  |  |

7d-glucose is added in increasing concentration,  $\alpha_2$  falls systematically to a value 3–4 times lower at the 1:11 concentration. This change must again be due to the effect of the glucose on the dynamics of the water molecules: the rotational dynamics of the glucose molecules are 1 order of magnitude slower, corresponding to  $\tau = 20$  ps at the 1:11 concentration, as determined from the measurements on natural glucose in D<sub>2</sub>O.<sup>5</sup> The further reduction in  $\alpha_2$  with the more hydrogenated sugar molecules, 2d<sub>66</sub>-glucose and 1d<sub>2</sub>-methylated glucose, may again reflect the increased contribution of the sugar to the scattering and thus give an indication of the magnitude of this contribution in the case of the 7d-glucose. The temperature dependence of  $\alpha_2$  for the glucose solutions gives an average activation energy for orientational diffusion of  $1.8 \pm 0.08$  kcal mol<sup>-1</sup>, similar to the TBCD value for water of  $1.85$  kcal mol<sup>-1</sup>.<sup>9</sup>

The values of  $\beta_2$  follow a trend similar to those of  $\beta_1$  in Figure 6, with a comparable activation energy but systematically higher by about 0.06 meV, consistent with the increasing contribution of higher rotational terms as  $Q$  increases.

**D. Comparison with Previous Work on Sugar Solutions.** In QENS measurements on sucrose solutions, Feeney et al.<sup>8</sup> found a slowing down of the diffusion by a factor  $4 \pm 1$  on going from pure water to a 1:7 solution of natural D-fructose in D<sub>2</sub>O at 300 K, with jump diffusion becoming evident for compositions of 1:25 and 1:7, a somewhat smaller effect than observed here. Magazù et al.<sup>12</sup> obtained diffusion constants of  $1.6\text{--}1.8 \times 10^{-5}$  cm<sup>2</sup> s<sup>-1</sup> for 1:20 solutions of the disaccharides trehalose, maltose, and sucrose at the rather high temperature of 50 °C. Extrapolation of the results of ref 9 would imply a diffusion constant of  $7.0 \times 10^{-5}$  cm<sup>2</sup> s<sup>-1</sup> for pure water, so that the sugars are again slowing down the dynamics by a factor 4. Neither ref 8 nor ref 12 addresses the rotational dynamics of the water.

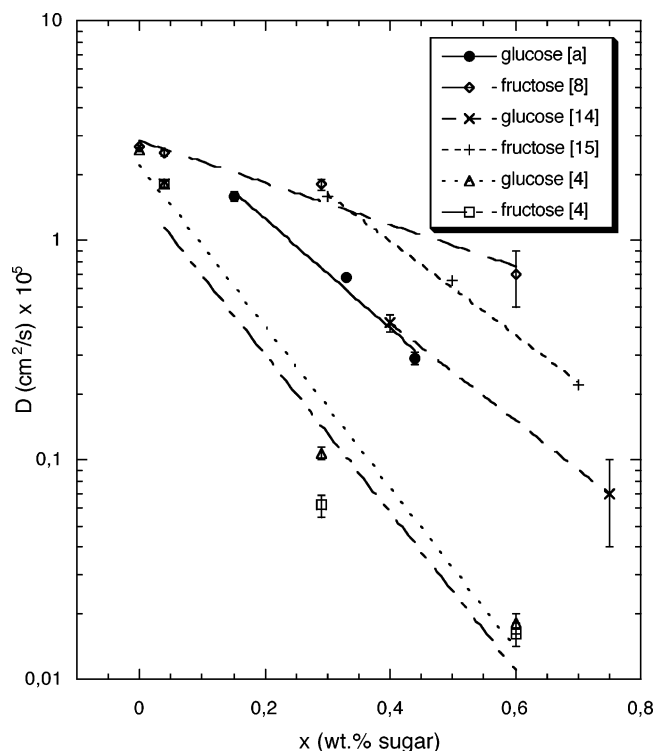


**Figure 7.** Values of the diffusion constant for water at 300K in monosaccharide solutions from present work [a] and experimental<sup>8,14,15</sup> and simulation<sup>4</sup> papers in the literature. The lines represent fits of exponential functions of the sugar concentration. [a] refers to the present work and the numbers in brackets to references in the text.

Other experimental techniques such as NMR and dielectric spectroscopy provide dynamical information complementary to QENS.<sup>13</sup> <sup>2</sup>H NMR has been used by Moran and Jeffery<sup>14</sup> to study the amorphous glass and liquid phases of glucose–water and by Rampp et al.<sup>15</sup> to study fructose–water solutions. Roberts and Debenedetti<sup>4</sup> have carried out molecular dynamics simulations on glucose and fructose solutions. In Table 3, we compile the experimental and simulation results on the diffusion of water in monosaccharide solutions, and in Figure 7, we display the values at 300 K. It can be seen that the QENS and NMR results are in good agreement, with the water diffusion constants being 3–4 times lower in the glucose solutions than the fructose solutions. The MD results for both are an order of magnitude below the experimental values, presenting a challenge for future computational work in this field.

It is not straightforward to compare orientational correlation times measured by NMR, dielectric spectroscopy, and QENS, but Moran & Jeffery<sup>14</sup> find values for T1 and T2 associated with orientational diffusion of water molecules of about 10 and 20 ps, respectively, for 40 and 75 wt % glucose–water solutions, consistent with the values of  $\tau$  we obtain by QENS. By comparing dielectric measurements on the same solutions, Moran et al.<sup>16</sup> conclude that the orientational motions take place by small jumps, in line with the model of freely rotating molecules introduced above to describe the QENS data.

## V. Conclusions

The principal finding of this work is that the addition of glucose to water in increasing concentration causes a systematic slowing down of the dynamics of the water molecules, by a factor of 10 for the translational diffusion and 3–4 for the rotational motions at the highest concentration studied, 1:11 C<sub>6</sub>H<sub>12</sub>O<sub>6</sub>:H<sub>2</sub>O, corresponding to 48 w/w % in the fully pro-

tonated solution. The inverse experiment, studying the dynamics of predominantly hydrogenated glucose in D<sub>2</sub>O on a backscattering spectrometer,<sup>5</sup> found an accompanying slowing down of the diffusion of the glucose molecules, by a factor 4 in going from the 1:55 to 1:11 concentration. Together with the NMR<sup>14</sup> and dielectric spectroscopy<sup>16</sup> work, these results present a rather complete picture of the dynamics of glucose–water solutions at temperatures above the melting point. In future work, we plan to investigate the supercooled liquids down to the glass transition with neutron backscattering and spin–echo spectroscopy. It would also be interesting to compare the two pure anomers ( $\alpha$  vs  $\beta$  methylated forms) or single anomer methylated sugars which differ at another, nonmutarotating position, like C2 (mannose) or C4 (galactose).

Numerical simulations of these complex liquids remain a challenge, and we hope that the present data can be used to validate different assumptions made in the calculations.

**Acknowledgment.** This work was supported by the U.S. National Institutes of Health, the U.S. Department of Energy, Office of Science, under Contract No. W-31-109-ENG-38, and the Centre National de la Recherche Scientifique, and utilized facilities supported in part by the National Science Foundation under Agreement No. DMR-0086210. We thank D. Neumann, P. E. Mason, and J. E. Enderby for helpful discussions. D.L.P. thanks the IPNS Division at Argonne National Laboratory, and M.L.S. thanks the James Franck Institute at the University of Chicago, for hospitality during the preparation of the manuscript.

The use of certain trade names or commercial products does not imply any endorsement of a particular product, nor does it imply that the named product is necessarily the best product for the stated purpose.

## References and Notes

- (1) Schmidt, R. K.; Karplus, M.; Brady, J. W. *J. Am. Chem. Soc.* **1996**, *118*, 541–546.
- (2) Liu, Q.; Brady, J. W. *J. Am. Chem. Soc.* **1996**, *118*, 12276–12286.
- (3) Sidhu, K. S.; Goodfellow, J. M.; Turner, J. Z. *J. Chem. Phys.* **1999**, *110*, 7943–7950.
- (4) Roberts, C. J.; Debenedetti, P. G. *J. Phys. Chem. B* **1999**, *103*, 7308–7318.
- (5) Smith, L. J.; Price, D. L.; Chowdhuri, Z.; Brady, J. W.; Saboungi, M.-L. *J. Chem. Phys.* **2004**, *120*, 3527.
- (6) Copley, J. R. D.; Cook, J. C. *Chem. Phys.* **2003**, in press.
- (7) The IDL-based DAVE suite of programs was used to derive the scattering functions  $S(Q, E)$  (<http://www.ncnr.nist.gov/dave/>).
- (8) Feeney, M.; Brown, C.; Tsai, A.; Neumann, D.; Debenedetti, P. B. *J. Phys. Chem. B* **2001**, *105*, 7799.
- (9) Teixeira, J.; Bellissent-Funel, M.-C.; Chen, S.-H.; Dianoux, A. J. *Phys. Rev. A* **1985**, *31*, 1913.
- (10) Singwi, K.; Sjölander, A. *Phys. Rev.* **1960**, *119*, 863. Egelstaff, P. A. *An Introduction to the Liquid State*; Clarendon: Oxford, U.K., 1992.
- (11) Sears, V. F. *Canad. J. Phys.* **1966**, *44*, 1299; **1966**, *45*, 237.
- (12) Magazù, S.; Villari, V.; Migliardo, P.; Maisano, G.; Telling, M. F. *J. Phys. Chem. B* **2001**, *105*, 1851.
- (13) Price, D. L.; Saboungi, M.-L.; Bermejo, F. J. *Rep. Prog. Phys.* **2003**.
- (14) Moran, G. R.; Jeffery, K. R. *J. Chem. Phys.* **1999**, *110*, 3472.
- (15) Rampp, M.; Buttersack, C.; Lüdermann, H. D. *Carbohydr. Res.* **2000**, *328*, 561.
- (16) Moran, G. R.; Jeffrey, K. R.; Thomas, J. M.; Stevens, J. R. *Carbohydr. Res.* **2000**, *328*, 573.